Applied Surface Science 255 (2008) 157–159

Contents lists available at ScienceDirect

Applied Surface Science

journal homepage: www.elsevier.com/locate/apsusc

Simulation of positron annihilation response to mechanical deformation of nanostructured Ni_3Al

O. Melikhova [a,b,*], J. Kuriplach [a], I. Prochazka [a], J. Cizek [a], M. Hou [b], E. Zhurkin [b,c], S. Pisov [b,d]

[a] Department of Low Temperature Physics, Faculty of Mathematics and Physics, Charles University in Prague, V Holesovickach 2, CZ-180 00 Prague 8, Czech Republic
[b] Physique des Solides Irradiés et des Nanostructures CP234, Université Libre de Bruxelles, Bd du Triomphe, B-1050 Bruxelles, Belgium
[c] Department of Experimental Nuclear Physics, Physical & Mechanical Faculty, K-89, St. Petersburg State Polytechnical University, 29 Polytekhnicheskaya Street, 195251 St. Petersburg, Russia
[d] Faculty of Physics, University of Sofia, 5 James Bourchier Street, 1164 Sofia, Bulgaria

ARTICLE INFO

Article history:
Available online 23 May 2008

PACS:
78.70.Bj
71.15.Pd
61.46.Hk

Keywords:
Positron annihilation
Molecular dynamics
Open volume defects
Deformation
Nanowires

ABSTRACT

Simulations of the positron response to the mechanical deformation of Ni_3Al nanowires are performed on modelled samples obtained using molecular dynamics. Particular attention is paid to the evolution of the various open volume defects and their interaction during deformation. Positron simulations are done in conjunction with a general, geometrical analysis of open volumes in the studied samples, which brings complementary information to the positron response results.

1. Introduction

Deep understanding of deformation mechanisms and the role of defects upon loading are essential in order to control mechanical properties of materials. Considering high difficulties to investigate experimentally deformation mechanisms at the nanoscale, modelling is particularly attractive. In this work, Ni_3Al samples modelled by molecular dynamics (MD) using two different potentials are investigated in detail with respect to created open volume defects and their evolution during deformation. The possibility to resolve different types of defects and to follow their evolution experimentally by means of positron annihilation lifetime spectroscopy (PALS) is examined in the present work. There were numerous studies of nanostructured materials by means of positron annihilation (see e.g. [1]) and recently first positron experiments on nanowires/nanorods were also performed (see e.g. [2]). Simulations of the positron response of nanostructured materials were also carried out (see e.g. [3]) in order to help understanding the relation of measured positron characteristics and microscopic models of such materials.

2. Samples

Two crystalline Ni_3Al nanowires with $L1_2$ structure were chosen for investigation. They were modelled as cylinders with their axis along the [0 0 1] direction and with an initial diameter of 6.5 nm. In order to model cylindrical wires of an infinite length, a periodic boundary condition was applied in the [0 0 1] direction. They were deformed by a tensile uniaxial stress applied along the [0 0 1] direction at 300 K. The first nanowire, marked as sample A, was modelled using the second moment approximation of the tight binding model potential described in [4] with the parameterization suggested in [5]. The second nanowire, marked as sample B, was modelled using the embedded atom model [6] with functionals of Ref. [7]. Associated equilibrium lattice constants for samples A and B were $a_A = 3.567$ Å and $a_B = 3.618$ Å, respectively. The experimental value of the Ni_3Al lattice constant is 3.568 Å [8]. The structural evolution of each sample with the strain

* Corresponding author at: Department of Low Temperature Physics, Faculty of Mathematics and Physics, Charles University in Prague, V Holesovickach 2, CZ-180 00 Prague 8, Czech Republic. Tel.: +420 2 21912769; fax: +420 2 21912567.
E-mail address: oksivmel@yahoo.com (O. Melikhova).

0169-4332/$ – see front matter © 2008 Elsevier B.V. All rights reserved.
doi:10.1016/j.apsusc.2008.05.291

($\varepsilon_{zz} = (l - l_0)$, where l_0 and l are the lengths of the sample before and after deformation, respectively) was followed by deformation steps $\Delta\varepsilon_{zz} = 0.05$ until rupture. The detailed description of the sample preparation procedure and deformation experiment can be found in Ref. [9].

3. Computational analysis methods

Analyses of free volumes (FVs) were made by means of the FREEVOL program [10]. Parameters' setting in FREEVOL was done in order to allow detecting open volumes of about 7 Å^3 (~0.6 of single vacancy size) and larger. FVs distributions were found multimodal and corresponding FV groups were distinguished statistically according to the following rule: only FVs in a mode with sizes that do not differ by more than three standard deviations from the mean value of this mode were included in the same group.

Positron annihilation lifetimes (PALs) were calculated by means of the ATSUP program [3,11] based on the atomic superposition method [12,13]. Both FREEVOL and ATSUP codes were updated in order to allow handling nanowires. Surface positron states were not considered.

For simulations of PAL spectra corresponding to modelled samples a Monte Carlo technique was employed. Given the positron lifetimes and trapping rates for each type of defect, a PAL spectrum was computer generated[1] considering the scheme of the simple trapping model (STM) [14]. Convolution of the spectrum with a time resolution function was involved in the simulations. The resolution function consisted of 3 Gaussians leading to the total full width at half maximum of 170 ps. Such a resolution function is provided by the positron lifetime spectrometer at the Charles University in Prague [15]. Each simulated spectrum contained $\approx 10^7$ counts. The source contribution to annihilation spectra (^{22}Na between mylar foils) was modelled by two components with lifetimes $\tau_{s1} = 368$ ps and $\tau_{s2} = 2$ ns and corresponding intensities $I_{s1} = 8\%$ and $I_{s2} = 2\%$, respectively. Simulated spectra were finally decomposed by means of a maximum-likelihood procedure [16].

4. Results

4.1. Analyses of FV

During plastic deformation, two groups of FVs were distinguished in the sample A. The first group ("FV1" in what follows) is the distribution of vacancy-like defects at grain boundaries (GBs) with the size 7–22.5 Å^3 (0.6–2 vacancies). The second group (FV2) is a single cluster with the size ranging from 42 Å^3 to 422 Å^3 (~4–40 vacancies) depending upon the magnitude of deformation. This cluster appears at GBs for some extensions. In the case of the sample B only the group FV1 with the size 7–25.5 Å^3 (0.6–2 vacancies) was found. The evolution of the mean FV and total FV1 for both samples is shown in Fig. 1.

Neither the mean FV size nor the total volume of the group FV1 display any clear evolution during the deformation of the sample A. Defects of this group do not diffuse between different GBs, however, they may diffuse within GBs. No defects were found inside grains of the sample A. In the case of the sample B, the mean FV size for the distribution FV1 displays no clear evolution during the deformation whereas the total volume of the distribution increases at the beginning of plastic deformation. So far, defects are only detected at GBs. At strains larger than $\varepsilon_{zz} = 0.3$, defects were also found inside grains because of the onset of a structural

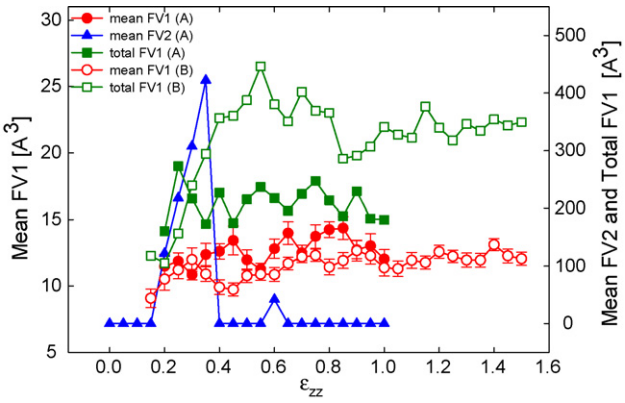

Fig. 1. The mean FV1 (circles), FV2 (triangles) and total FV1 (squares) versus strain for sample A (filled symbols) and sample B (empty symbols).

transformation ($L1_2$ to tetragonal; see Ref. [9] for details), which caused a further increase in the total FV1. Beyond this structural transformation, at strains larger than $\varepsilon_{zz} = 0.85$, defects are mainly found inside grains and defects' positions remain stable upon further deformation. The total volume of the FV1 distribution levels off until rupture. The width of the FV1 distribution remains constant during deformation for both samples.

At the smallest plastic deformation of the sample A, one cluster (FV2) appears at the boundary between two grains. The position of its centre of mass remains stable and this cluster grows up during deformation. A kink develops at the surface and annihilates the cluster at $\varepsilon_{zz} = 0.4$. At $\varepsilon_{zz} = 0.6$ a new cluster (FV2) appears due to the migration and the coalescence of three defects from group FV1. It annihilates the same way as the previous one at $\varepsilon_{zz} = 0.65$. This indicates that the sample surface plays an important role in deformation mechanisms and serves as a sink for large defects.

4.2. Simulation of the positron response

Considering a large amount of defects in each sample (usually a few tens) occurring at each extension examined, calculating PALs for each individual defect by the ATSUP program would be unpractical. For this reason, we assume that positrons in FV defects have the same lifetime as in spherical defects of the same size. The lifetime corresponding to a given FV in modelled samples was estimated by interpolation between lifetimes in vacancy clusters. The latter were prepared in the following way. Clusters up to 15 vacancies were created by removing individual atoms from a $4 \times 4 \times 4$ lattice unit $L1_2$ Ni_3Al supercell. Larger vacancy clusters were constructed by omitting gradually coordination shells of a reference atom (Al) from a $10 \times 10 \times 10$ lattice unit $L1_2$ Ni_3Al supercell, up to the 17th coordination shell. Calculated dependencies of PALs for such vacancy clusters were done for both lattice constants a_A and a_B.

Different lattice constants result in practically no difference in the dependence of the PAL on the volume of defects. Approximated values of PALs differ from those calculated with ATSUP for selected defects in samples by no more than 10 ps, when defects with the same volumes are considered. This difference can be caused, on the one hand, by FV shapes that may deviate from a sphere, and on the other hand, by the limited precision of the FV size calculation by FREEVOL.

When simulating PAL spectra, the trapping rate was assumed to be proportional to the volume fraction of the defect [17], with the proportionality constant $\mu_{1V} = 2.8 \times 10^{15}$ s^{-1} [18] defining the specific trapping rate for single vacancies in Ni_3Al.

[1] Unpublished code. FORTRAN source file is available from authors.

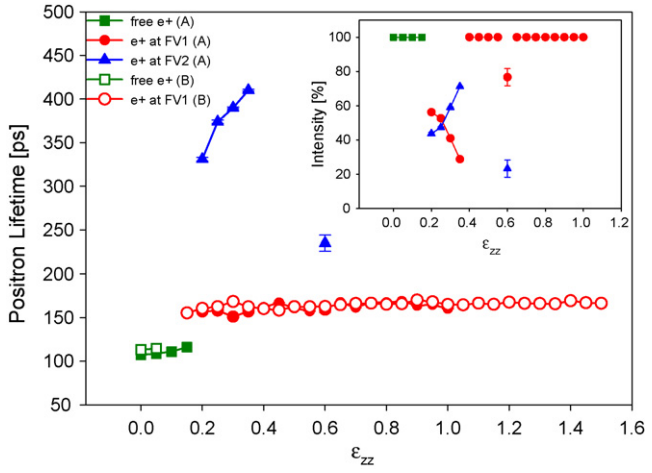

Fig. 2. The evolution of PALs and their intensities during deformation of sample A (filled symbols) and of sample B (empty symbols). Squares: free positrons; circles: positrons trapped at FV1; triangles: positrons trapped at FV2.

4.3. Decomposition of simulated spectra

Simulated spectra were decomposed into three or four (for some extensions of the sample A) exponential components including the source contribution. PALs of source components τ_{s1} and τ_{s2} and the intensity I_{s1} were fixed to the above mentioned values during decomposition. Consistency of the fitted model with the simulated spectra was observed in all cases, χ^2-values being typically (1.00 ± 0.03). The evolution of PALs and of their intensities during deformation is shown in Fig. 2.

Bulk PALs calculated for the $4 \times 4 \times 4$ lattice unit $L1_2$ Ni_3Al supercells with lattice parameters a_A and a_B are 104.5 ps and 109 ps, respectively. Due to temperature effects PALs calculated before deformation of samples A and B are 107 ps and 113 ps, respectively. In both, the PAL of free positrons slightly increases with the strain during elastic deformation and saturation trapping occurs during plastic deformation due to the high concentration of defects.

The shortest component obtained by the fit, τ_1, corresponds to positrons trapped at vacancy-like defects of the group FV1. For simulations of spectra, rather wide distributions of lifetimes from 137 ps to 194 ps (sample A) and from 144 ps to 201 ps (sample B) were used, resulting in decomposed lifetimes 151–169 ps. No evolution of τ_1 was seen during deformation. Individual defects inside the group FV1 cannot be resolved in PAL spectra.

The second fitted component, τ_2, represents positrons trapped at vacancy clusters of the group FV2 (sample A). A single lifetime was used for the spectrum simulation. This lifetime was estimated for the single cluster which appeared at some extensions (see Fig. 1). The fitted lifetime reproduces very well the simulated value. Changes in the FV2 cluster size can be seen in an increase of the lifetime value as well as in an increase of the intensity of the second component. The coalescence of FV1 defects resulting in a FV2 cluster at the elongation $\varepsilon_{zz} = 0.6$ with an estimated PAL of 245 ps can be also resolved in the PAL spectrum, but with a worse reproduction of the simulated value (fitted lifetime $\tau_2 = 235 \pm 9$ ps) due to proximity of the first component.

5. Conclusions

Associating atomic scale modelling – that provides detailed information about the state of the sample during deformation – with the simulations of PAL spectra for the same model sample allows to assess which part of this information could be resolved in PAL experiments. Simulations indicate that a single lifetime cannot be assigned to trapping sites at GBs, but such defects are rather represented by a distribution from which a weighted average value can only be found in PAL measurements. Even if individual defects are irresolvable, detected components of PAL spectra reflect well the evolution of different groups of FV defects in studied samples. Hence, the positron response can be useful for the identification of open volume defects and investigation of their behaviour during deformation. It should also be mentioned that there are apparent differences in FV and PAL characteristics of larger free volumes (FV2) for the samples simulated with different MD potentials, but otherwise same conditions. PAL measurements can be thus foreseen as a qualitative tool to assess the adequacy of potentials used for simulations of Ni_3Al nanowires.

Acknowledgments

We are grateful to M.J. Puska for his ATSUP code that served as a basis for further developments. OM is thankful for a grant of the Université Libre de Bruxelles and of the Fonds National de la Recherche Scientifique of Belgium, under agreement 2.4520.03F. SP is grateful to the Science Policy Office of the Federal Government of Belgium for a grant in the frame of the IAP 5-1 project "Quantum size effects in nanostructured materials". This work is part of the research plan MS 0021620834 and the project COST OC165 supported by the Ministry of Education of the Czech Republic. The presented research is also carried out within the framework of the COST Action P19 "Multiscale Modelling of Materials". This research is supported by the Grant Agency of the Czech Republic (project No. 202/06/1509).

References

[1] R. Würschum, M. Scheytt, H.E. Schaefer, Phys. Status Solidi A 102 (1989) 119.
[2] G. Brauer, W. Anwand, D. Grambole, W. Skorupa, Y. Hou, A. Andreev, C. Teichert, K.H. Tam, A.B. Djurisic, Nanotechnology 18 (2007) 195301.
[3] J. Kuriplach, et al. Mater. Sci. Forum 363–365 (2001) 94.
[4] G.J. Ackland, V. Vitek, Phys. Rev. B 41 (1990) 10324.
[5] F. Gao, D. Bacon, G. Ackland, Philos. Mag. A 67 (1993) 275.
[6] S.M. Foiles, M.I. Baskes, M.S. Daw, Phys. Rev. B 33 (1986) 7983.
[7] R.A. Johnson, Phys. Rev. B 41 (1990) 9717.
[8] L.-S. Hsu, Y.K. Wang, G.Y. Guo, J. Appl. Phys. 92 (2002) 1419.
[9] M. Hou, O. Melikhova, S. Pisov, Mechanical properties of bimetallic crystalline and nanostructured nanowires, Faraday Discuss. 138 (2008), p.59.
[10] J. Kuriplach, Appl. Surf. Sci 194 (2002) 61.
[11] J. Kuriplach, Acta Phys. Pol. A 107 (2005) 784.
[12] M.J. Puska, R.M. Nieminen, J. Phys. F: Met. Phys 13 (1983) 333.
[13] A.P. Seitsonen, M.J. Puska, R.M. Nieminen, Phys. Rev. B 51 (1995) 14057.
[14] P. Hautojärvi, C. S Corbel, in: A. Dupasquier, A.P. Mills (Eds.), Proceedings of the International School of Physics "Enrico Fermi" Course CXXV, IOS Press, Varena, 1995, p. 491.
[15] F. Becvar, J. Cizek, L. Lestak, I. Novotny, I. Prochazka, F. Sebesta, Nucl. Instrum. Methods Phys. Res. A 443 (2000) 557.
[16] I. Prochazka, I. Novotny, F. Becvar, Mater. Sci. Forum 255–257 (1997) 772.
[17] R.M. Nieminen, J. Laakkonen, Appl. Phys. 20 (1979) 181.
[18] S. Van Petegem, E.E. Zhurkin, W. Mondelaers, C. Dauwe, D. Segers, J. Phys., Condens. Matter 16 (2004) 591.